

Application of the RAPID Fission Matrix Methodology to 3-D Whole-core Reactor Transport

William J. Walters*

*Mechanical and Nuclear Engineering Department, Penn State University, University Park, PA
wwalters@psu.edu

Abstract - In this paper, the RAPID fission matrix methodology, previously developed for spent fuel pool analysis, is tested for effectiveness on reactor problems. Several cases are examined, based on the NEA/OECD Monte Carlo Performance Benchmark Problem. In the RAPID methodology, fission matrix coefficients are pre-calculated using the Serpent Monte Carlo code, which were then coupled together and solved for different core arrangements. A new boundary correction method was added to obtain more accurate fission matrix values near the radial and axial reflectors. Eigenvalues and fission source distributions are compared between RAPID calculations and Serpent. In all cases, the eigenvalue differences between methods were less than 100 pcm. Pin-wise fission distributions between the methods differed on average between 1-2%, similar to the Monte Carlo uncertainty. To achieve these levels of uncertainty, the RAPID calculations were over 100 times faster than Serpent, not counting the pre-calculation time.

I. INTRODUCTION

Currently, the Monte Carlo method is the gold standard for neutronics calculations due to the ability to use exact geometry and continuous energy and angle variables, unlike deterministic methods. However, there are some significant limitations, especially when it comes to full-core reactor eigenvalue calculations. The first is in the quantity of information. Ideally, power distributions would be available at the pin or sub-pin level, with many axial levels per pin. To obtain this level of information with a reasonable statistical uncertainty with the Monte Carlo method is currently exceedingly difficult. In addition to this, there is the much more subtle and potentially difficult issue of source convergence. It is very difficult to tell when the fission source has converged, and tallies obtained may have questionable uncertainties due to auto-correlation between generations.

One technique to alleviate some of the issues of Monte Carlo eigenvalue calculations is the use of the fission matrix method. This has seen an increase in popularity lately, with the ability to improve convergence, accuracy, and speed of such calculations[1, 2, 3].

Recently, the RAPID (Real-time Analysis for Particle-transport and in-situ Detection) code was developed[4, 5, 6] which combines pre-calculated fission-matrix coefficients to solve subcritical multiplication or eigenvalue problems. It was originally developed for spent fuel pool calculations, which are especially troublesome for the Monte Carlo eigenvalue method. In this paper, it is extended for use in reactor geometry, and tested on the NEA Monte Carlo Performance Benchmark problem[7].

II. RAPID DESCRIPTION

The fission matrix method for an eigenvalue problem the fission source in cell i is given by Equation (1).

$$F_i = \frac{1}{k} \sum_{j=1}^N a_{i,j} F_j \quad (1)$$

Where F_j is the induced fission source strength in spatial

cell j , $a_{i,j}$ is the number of neutrons directly produced in spatial cell i due to a fission neutron born in cell j , and k is the fundamental eigenvalue. N is the total number of computational cells (which could be a whole assembly, a single fuel pin, or a fraction thereof). This can also be written in matrix form as below.

$$F = \frac{1}{k} \mathbf{A}F \quad (2)$$

Where, F is the fission source vector containing the N source values, and \mathbf{A} is the "fission matrix" that holds the $a_{i,j}$ values.

The fission matrix method results in a set of N linear equations, which can be solved for F and k given the $a_{i,j}$ coefficients. The chief difficulty is how to calculate the coefficients, and to decide on a computational cell size that is small enough to give detailed and accurate results, but not so large that the linear system becomes intractable. This can happen quickly as the matrix is of size $N \cdot N$. For a PWR system with 241 fuel assemblies, 264 fuel pins, and 100 axial levels, this is over 6 million cells, and 4×10^{13} total elements in the matrix. However, most of these coefficients will be close to zero due to the long distance between cells. A large fraction of values are also nearly identical due to geometric similarity. These factors are both taken into account in RAPID to reduce memory storage requirements and computation time.

1. Boundary Correction Factor

In general, RAPID assumes a similarity in fission matrix coefficients between similar assemblies, regardless of their location within the core. In previous studies on spent fuel applications, this was generally a good approximation due to the presence of strong absorbers surrounding all assemblies. In reactor applications however, the radial reflector causes a fairly large change in behavior. In order to account for this, a boundary correction factor was added. To generate the boundary correction factor, the standard model of the system is run with a uniform fixed source in the fuel, with fission turned off, and the fission neutron production rate is tallied in all pins, yielding $f(x, y)$. Next, a new model with and infinite

array of assemblies (i.e., no radial reflector) is run using the same fixed source, yielding $\tilde{f}(x, y)$. The boundary correction factor is then calculated as a simple ratio as in Equation (3).

$$bnd(x, y) = f(x, y) / \tilde{f}(x, y) \quad (3)$$

This factor can then be applied to fission matrix coefficients near the boundary as in Equation (4).

$$a_{i,j} = bnd(x_i, y_i) \tilde{a}_{i,j} \quad (4)$$

Here, $\tilde{a}_{i,j}$ is the uncorrected fission matrix value, and x_i, y_i is the x, y location of cell i .

An similar process was performed in the axial (z) direction to obtain a full (x, y, z) boundary correction.

III. BENCHMARK DESCRIPTION

The NEA Monte Carlo Performance benchmark was developed to help monitor the improvement of Monte Carlo code performance over time, and to motivate improvements in Monte Carlo codes and implementation. One goal of the benchmark is to obtain local pin-wise, axially dependent values, which is difficult for standard Monte Carlo, but should be a strong point of the RAPID fission matrix methodology.

In the benchmark, the reactor core consists of 241 identical fuel assemblies, with dimensions 21.41 x 21.42 cm². The X-Y core layout is shown in Figure 1. The core baffle plates and core barrel have been homogenized into a radial reflector region. This is surrounded by a downcomer region (inner radius 209 cm, outer radius 229 cm), followed by the reactor vessel (outer radius 249 cm).

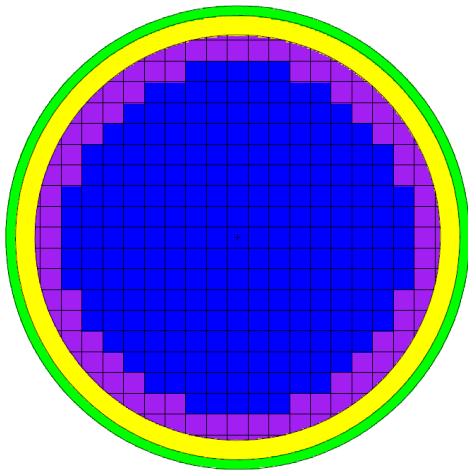


Fig. 1. X-Y reactor core layout. Fuel assemblies (blue) are surrounded by radial reflector (purple), then the downcomer region (yellow), and finally the reactor vessel (green)

In the Z-direction, the fuel has an active length of 366 cm. In order to add asymmetry to the problem, the coolant density changes from 0.76 g/cm³ in the bottom “cold” half of the core to 0.64 g/cm³ in the upper “hot” half of the core. There are three homogenized regions above and below the fuel that represent the bottom fuel assembly region, nozzle

region, and core plate region. An X-Z slice of the reactor core is shown in Figure 2.

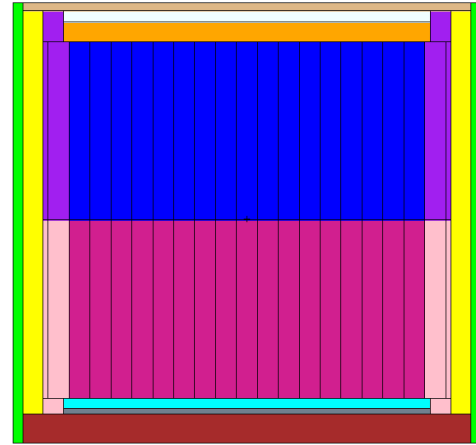


Fig. 2. X-Z reactor core layout. The upper half of the reactor has lower density “hot” coolant while the lower half has higher density “cold” coolant.

Each fuel assembly consists of 17x17 cells, with 264 fuel pins and 25 control/instrumentation tubes, as shown in Figure 3. The pin pitch is 1.26 cm. No spacers or other construction materials are modeled.

The fuel material is taken to represent roughly 24,000 MWd/ton burnup fuel with 17 actinides, 16 fission products and oxygen. Boron has been added to the coolant such that the reactor is near critical. For additional details on materials and dimensions, consult the benchmark document[7].

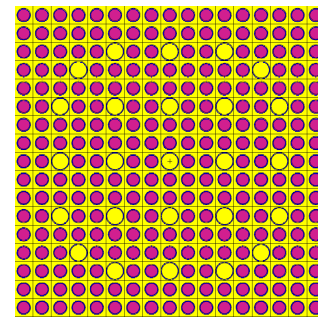


Fig. 3. 17x17 assembly with 264 fuel pins and 25 control/instrumentation tubes

In addition to the benchmark problem, several other cases were derived to test the performance in different scenarios. The first new case is a simple 2-D slice through the benchmark problem in the “cold” section. Next, a uniform case is added, which is like the benchmark but with cold moderator throughout (no axial variation). For the next two cases, a new fuel type was created with a 20% higher U-235 content. With this, two cases were added, one where the fuel material is changed to high enriched in the top half (axial case), and one with a radial variation in fuel assembly types. For both of these cases, cold moderator was used throughout. The layout of the high enriched assemblies in the radial case is shown in Figure 4.

An overview of all the cases is given in Table I.

TABLE I. Description of computational cases examined in this paper

| Case | Description |
|-------------------|---|
| Benchmark | As described by benchmark |
| Slice | 2-D model of a slice through the "cold" section |
| Uniform | As per benchmark, but with cold moderator throughout |
| Axial Enrichment | Cold moderator throughout, but top half higher U-235 concentration |
| Radial Enrichment | Cold moderator throughout, but half radially higher U-235 concentration in checkerboard |

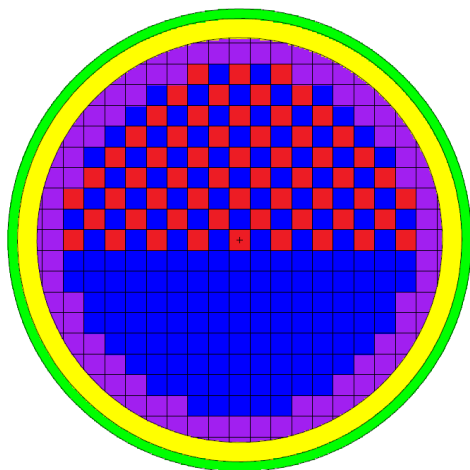


Fig. 4. X-Y reactor core layout for the radial modified case. The higher enriched assemblies are shown in red.

IV. RAPID COEFFICIENT DATABASE GENERATION

The first step for RAPID calculations is to create a database of fission matrix coefficients and boundary correction factors. This was done separately for each of the three assembly types used in the cases (i.e., the “hot”, “cold”, and “cold enriched” assemblies). A single fixed source calculation with 3,000,000 histories was performed for each fuel pin in a single octant of a fuel assembly (39), for each assembly type (3), for a total of 117 calculations. Fission neutron production was tallied in all surrounding pins as well as axially to yield the fission matrix coefficients. The total calculation time for these was 11.7 CPU-hours. The statistical uncertainty for the sum of the calculated coefficients from each pin was $\sim 0.05\%$. An example of the results from a single coefficient calculation is shown in Figure 5. For this application, coefficients are kept that are within 3 assembly pitches away from the source assembly.

For the boundary correction factor, two Serpent calculations were performed, one for the infinite case and one with the actual reflectors. From this, the (x,y) and (z) correction factors were extracted for both radial and axial reflector types. These calculations used 3×10^8 particle histories each, for a total of 20.9 CPU-hours. The uncertainty in the correction factor values is unclear, as correlated source sampling was used to obtain more accurate ratio values. A plot of the (x,y) boundary correction factors for the “hot” radial reflector is shown in Figure 6 for all ratio values > 1.005 . The correction is very large near the boundary but drops quickly to have no

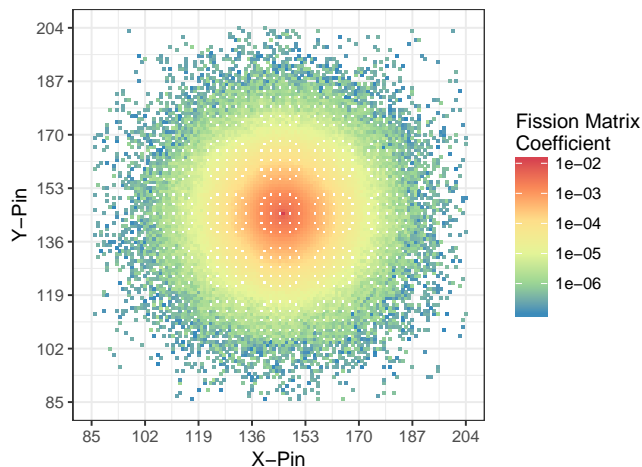


Fig. 5. Fission matrix coefficients calculated with Serpent for a single pin located at (146,145). Only values $> 10^{-7}$ are shown.

influence on assemblies not adjacent to the reflector.

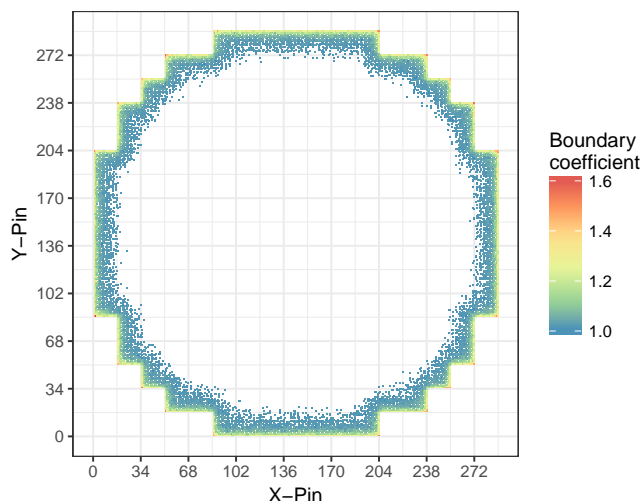


Fig. 6. (x,y) boundary correction factor for the “hot” radial reflector

In total, the RAPID pre-calculation time for database generation for this problem was 32.6 CPU-hours. This is a relatively short amount of time, and this single database is

used for all the different cases presented below. This contrasts to standard Monte Carlo, where the entire process must be repeated for any change in assembly arrangement. Fission matrix database generation can be seen as analogous to multi-group cross section generation in standard reactor analysis.

V. MONTE CARLO - RAPID COMPARISON

For each of the 5 cases (slice, standard benchmark, uniform, axial enrichment, radial enrichment) described earlier, a reference Serpent calculation was performed and compared to RAPID calculations. For RAPID, the same coefficient database was used for all cases. The main metrics to compare the methods are in eigenvalue, pin-wise fission uncertainty/error, and computation time. The pin-wise RAPID errors are calculated as mean of the absolute value of the relative difference between the Serpent and RAPID values. For both RAPID and Serpent, the fission distributions were obtained for every pin with 50 z-levels (~ 3, 000, 000 tallies).

1. 2D Slice Model

This model is a simple 2-D slice through the “cold” region of the benchmark. The Serpent model was run with 2,500,000 particles per cycle with 300 skipped cycles and 2500 active cycles. Fission distribution results are shown in Figure 7, and pin-wise uncertainties are in the range of 0.25-1%. The difference between the RAPID values and Serpent values are shown in Figure /reffig:sliceerr. This shows excellent agreement between the two codes, with most pin-wise differences being between -1 to 1%. There are some larger differences close to the reflector, both because of the approximate nature of the boundary correction, and because of the larger Monte Carlo uncertainty in those regions (over 1%). A comparison summary of the Serpent-RAPID differences is given in Table II. This shows the good agreement on k (59 pcm), the very low average pin-wise error, and much shorter RAPID computation time.

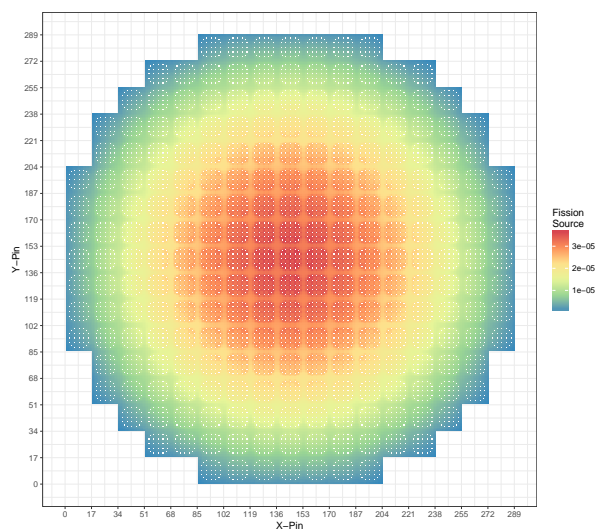


Fig. 7. Pin-wise fission source distribution for the slice model

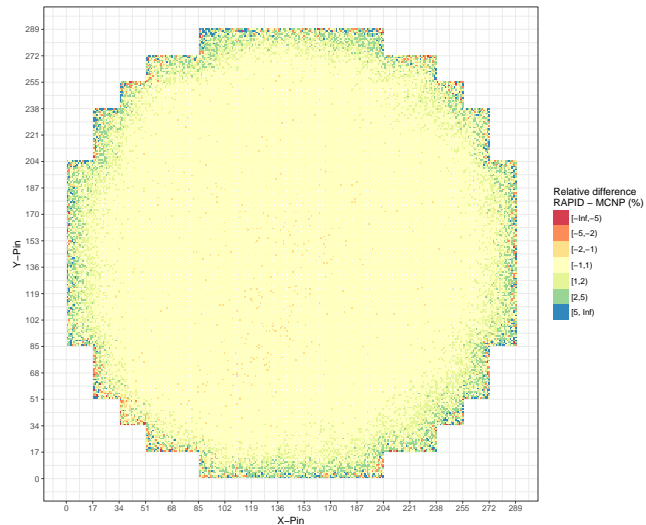


Fig. 8. Pin-wise fission source difference between RAPID and Serpent calculations for the slice model

TABLE II. 2D Slice Model Serpent-RAPID Comparison

| | Serpent | RAPID |
|------------------------------|---------|---------|
| k-eigenvalue | 1.00449 | 1.00390 |
| Eigenvalue uncertainty/error | 1 pcm | -59 pcm |
| Pin-wise uncertainty/error | 0.40% | 0.60% |
| Computation time (CPU-hrs) | 318 | 0.2 |

2. Standard Benchmark Model

This model is the standard, unmodified NEA benchmark problem. The Serpent model was run with 500,000 particles/cycle, 300 skipped cycles and 2500 active cycles. Fission distribution results are shown in Figure 9. Pin-wise uncertainties were in the range of 0.75-2%. Differences between Serpent and RAPID results are shown in Figure 10. Again, these pin-wise differences are usually within a few percent, and are larger near the boundary. The axial distribution of fission source, shown in Figure 11 shows significant differences at the interface between hot and cold regions. This is due to the very different transport properties of the two regions, and RAPID cannot properly estimate the fission matrix coefficients from hot to cold and vice-versa. This error did not go away with refinement of the axial mesh size. However, this drastic change in moderator density is not physically realistic, and RAPID is capable of handling fuel material differences but better than moderator differences, as will be shown in the radial and axial enrichment model cases. The pin-wise axial variation of the fission source is shown for two pins (near the outside, one near the middle of the core) in Figure 12. This shows the very large uncertainties at the detailed level for Monte Carlo tallies, which is a key strength of the RAPID method. A summary of the results for this model is shown in Table III.

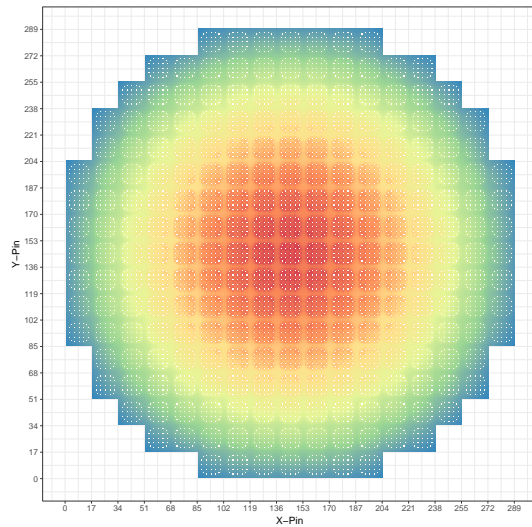


Fig. 9. Pin-wise fission source distribution for the standard benchmark model

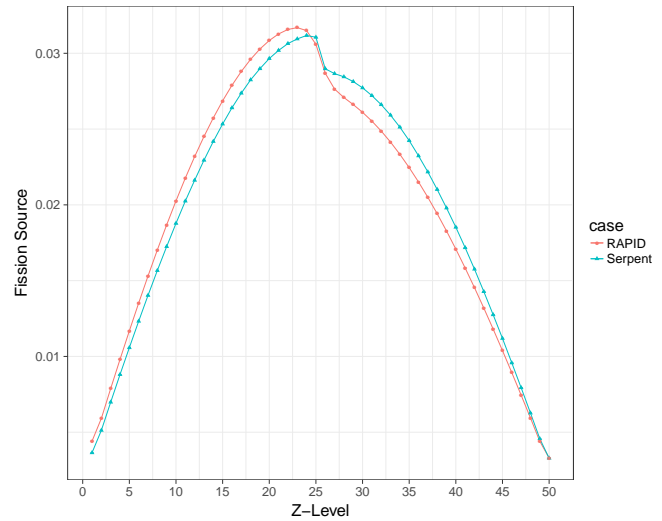


Fig. 11. Axial source distributions calculated by RAPID and Serpent for the standard benchmark model

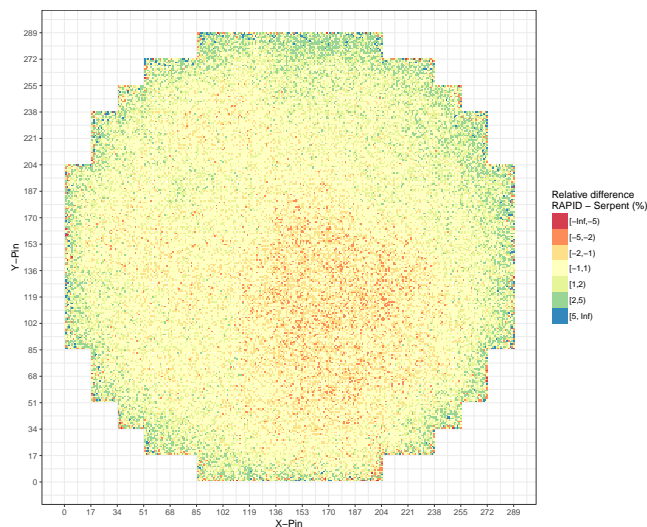


Fig. 10. Pin-wise fission source difference between RAPID and Serpent calculations for the standard benchmark model

TABLE III. Benchmark Model Serpent-RAPID Comparison

| | Serpent | RAPID |
|------------------------------|---------|----------|
| k-eigenvalue | 1.00074 | 0.99961 |
| Eigenvalue uncertainty/error | 5 pcm | -115 pcm |
| Pin-wise uncertainty/error | 0.91% | 1.05% |
| Computation time (CPU-hrs) | 67 | 0.4 |

3. Uniform Model

This model is like the standard model, except with the cold moderator used throughout the core. The upper axial/radial reflectors still contain the hot moderator density. Serpent transport parameters are identical to the benchmark model. Pin-wise fission and error distributions look similar to

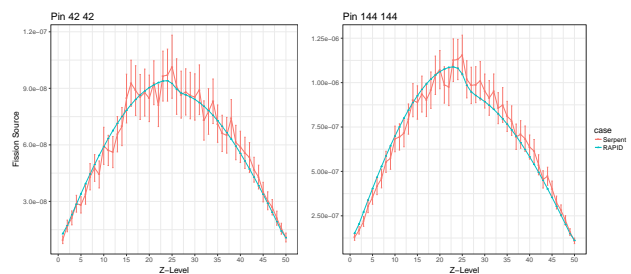


Fig. 12. Single pin axial source distributions calculated by RAPID and Serpent for the standard benchmark model

the previous case, so are not shown here. The axial distribution, as shown in Figure [reffig:coldz looks very good when only a single material is used. The pin-wise axial variation of the fission source is shown in Figure 14. A summary of the results for this model is shown in Table IV.

TABLE IV. Uniform Model Serpent-RAPID Comparison

| | Serpent | RAPID |
|------------------------------|---------|---------|
| k-eigenvalue | 1.00083 | 1.00010 |
| Eigenvalue uncertainty/error | 5 pcm | -73 pcm |
| Pin-wise uncertainty/error | 0.92% | 1.20% |
| Computation time (CPU-hrs) | 65 | 0.4 |

4. Radial Enrichment Model

This model again has only the cold moderator, and is uniform axially, but has several higher-enriched uranium assemblies in a checkerboard formation in half of the core, as shown in Figure 4. Serpent parameters are again the same, and the pin-wise fission source results are shown in Figure 15. There is a large skewing of source to the +y side of the core where the higher enrichment fuel is located. Differences between

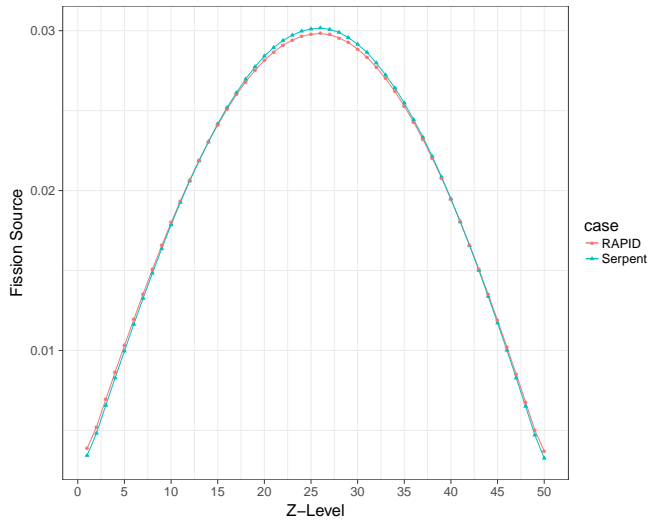


Fig. 13. Axial source distributions calculated by RAPID and Serpent for the uniform model

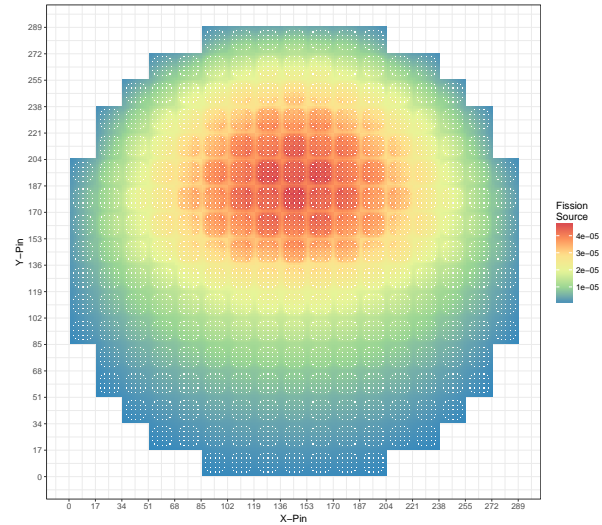


Fig. 15. Pin-wise fission source distribution for the radial enrichment model

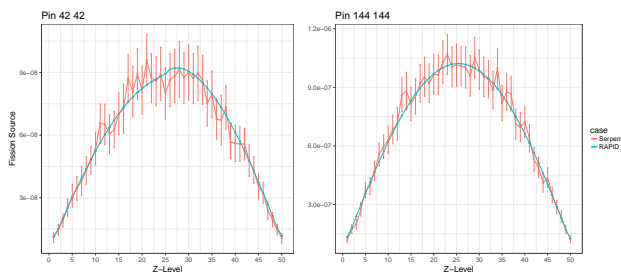


Fig. 14. Single pin axial source distributions calculated by RAPID and Serpent for the uniform model

Serpent and RAPID are shown in Figure 16, and show some larger differences at the interface between assembly types, but still overall accurate results. Axial source distributions, shown in Figure 17, are similar to the uniform case, as there is no axial material variation, and results again agree well. The pin-wise axial variation of the fission source is shown in Figure 18. A summary of the results for this model are shown in Table V.

TABLE V. Radial Enrichment Model Serpent-RAPID Comparison

| | Serpent | RAPID |
|------------------------------|---------|---------|
| k-eigenvalue | 1.01382 | 1.01295 |
| Eigenvalue uncertainty/error | 6 pcm | -85 pcm |
| Pin-wise uncertainty/error | 1.34% | 1.79% |
| Computation time (CPU-hrs) | 46 | 0.4 |

5. Axial Enrichment Model

This model uses only the cold moderator, but the upper half of the core uses entirely the higher-enriched fuel. The pin-wise fission source and RAPID error distributions are given in Figures 19 and 20. The axial distribution is given in Figure 21,

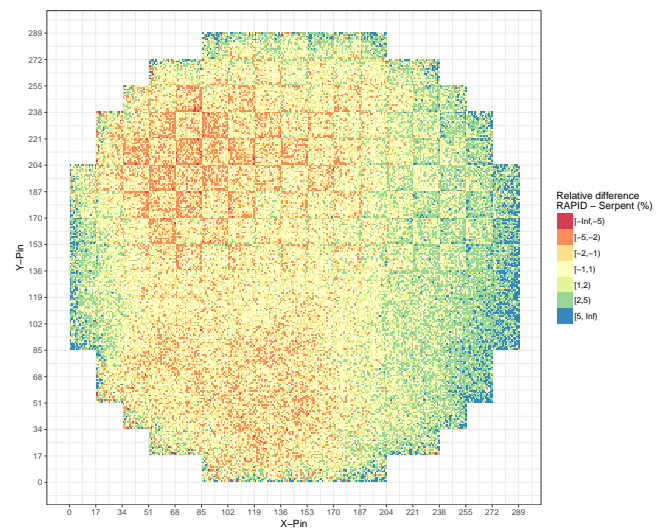


Fig. 16. Pin-wise fission source difference between RAPID and Serpent calculations for the radial enrichment model

and shows the large effect of the increased enrichment of the upper half of the core. RAPID shows good agreement with Serpent despite the abrupt change between material types at the core mid-plane. This is a contrast to the standard reference case with a change in moderator density at the mid-plane, where RAPID was not able to accurately estimate the coefficients between assembly types. A summary of the results for this model are shown in Table VI.

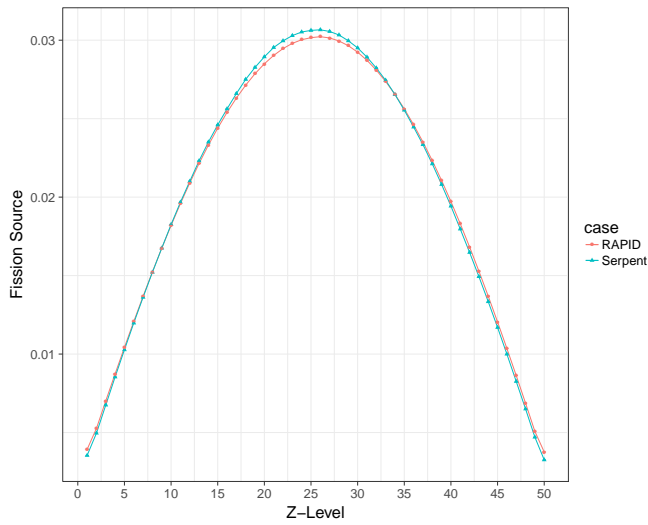


Fig. 17. Axial source distributions calculated by RAPID and Serpent for the radial enrichment model

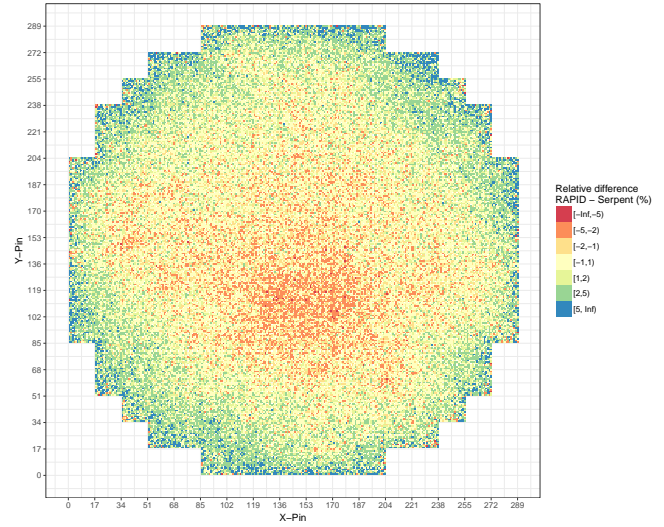


Fig. 20. Pin-wise fission source difference between RAPID and Serpent calculations for the axial enrichment model

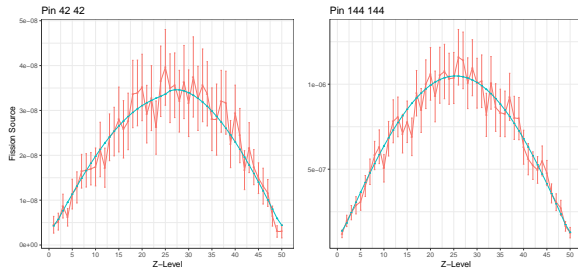


Fig. 18. Single pin axial source distributions calculated by RAPID and Serpent for the radial enrichment model

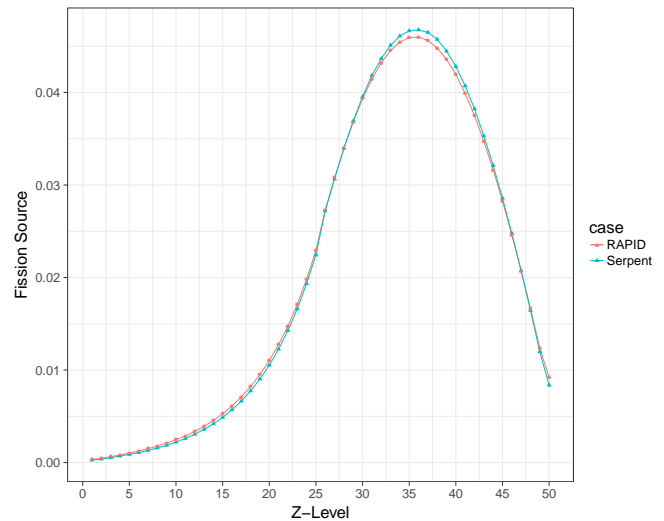


Fig. 21. Axial source distributions calculated by RAPID and Serpent for the axial enrichment model

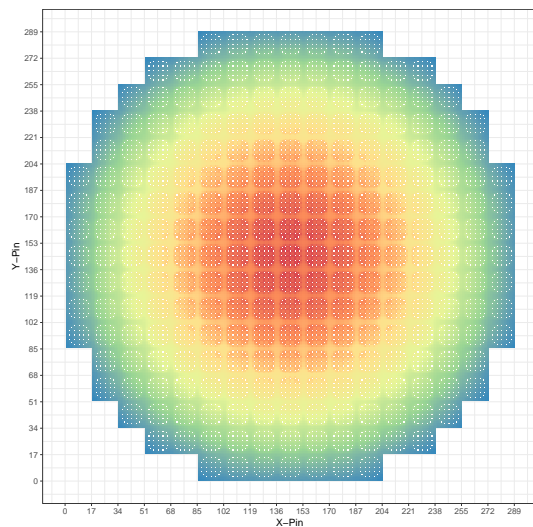


Fig. 19. Pin-wise fission source distribution for the axial enrichment model

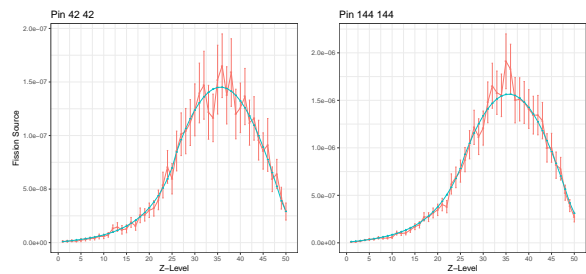


Fig. 22. Single pin axial source distributions calculated by RAPID and Serpent for the axial enrichment model

TABLE VI. Axial Enrichment Model Serpent-RAPID Comparison

| | Serpent | RAPID |
|------------------------------|---------|---------|
| k-eigenvalue | 1.02883 | 1.02791 |
| Eigenvalue uncertainty/error | 6 pcm | -89 pcm |
| Pin-wise uncertainty/error | 1.52% | 1.85% |
| Computation time (CPU-hrs) | 47 | 0.4 |

VI. CONCLUSIONS

A novel fission matrix-based method that was previously developed for spent fuel pool applications has been adapted applied to a reactor problem. We compared the results from the RAPID fission matrix code to a standard Serpent Monte Carlo calculation on the the NEA/OECD Monte Carlo Performance Benchmark along with several variations. Fission matrix coefficients were pre-calculated for the three assembly types using continuous energy Monte Carlo. The eigenvalues calculated using RAPID were within 100 pcm of the Serpent value for all cases examined. The addition of a boundary correction factor to RAPID was essential to obtain these results that had previously been on the order of several hundred pcm. Average pin-wise fission source rates differences were on the order of 1% for all cases, very similar to the Serpent uncertainty. One area of weakness that was noted with RAPID was in areas of abrupt change of moderator density, as is the case in the performance benchmark. While this instantaneous density change may be un-physical, it still bears noting for future development. The same database of coefficients was used for all cases, and could be used for many other variations without re-calculation. Computation time of RAPID compared to Serpent was reduced by a factor of about 100 if the pre-calculation cost is discounted. Further, the Monte Carlo statistical uncertainty for individual pins with axial bins was still extremely high, whereas the RAPID solution does not show statistical fluctuations.

REFERENCES

1. J. DUFEK and W. GUDOWSKI, "Fission matrix based Monte Carlo criticality calculations," *Annals of Nuclear Energy*, **36**[8], 1270–1275 (2009).
2. M. WENNER and A. HAGHIGHAT, "A Fission Matrix Based Methodology for Achieving an Unbiased Solution for Eigenvalue Monte Carlo Simulations," *Progress in Nuclear Science and Technology*, **2**, 886–892 (2011).
3. S. CARNEY, F. BROWN, B. KIEDROWSKI, and W. MARTIN, "Fission Matrix Capability for MCNP Monte Carlo," Tech. rep., LANL (2012), 1A-UR-12-24533.
4. W. J. WALTERS, N. ROSKOFF, K. K. ROYSTON, and A. HAGHIGHAT, "Use of the Fission Matrix Method for Solution of the Eigenvalue Problem in a Spent Fuel Pool," in "Proceedings of PHYSOR 2014, The Role of Reactor Physics toward a Sustainable Future," (2014), Kyoto, Japan, September 28-October 3, 2014.
5. W. J. WALTERS, N. J. ROSKOFF, and A. HAGHIGHAT, "A Fission Matrix Approach to Calculate Pin-wise 3-D Fission Density Distribution," in "Proceedings of M&C 2015, Nashville, USA, Apr. 19-23, 2015," (2015).
6. N. J. ROSKOFF, A. HAGHIGHAT, M. MILLET, and C. LEIDIG, "Benchmarking of the RAPID tool for a sub-critical facility," in "Proc. 57th INMM annual meeting, Atlanta, GA, July 24-28," (2016).
7. J. E. HOOGENBOOM, W. R. MARTIN, and B. PETROVIC, "Monte Carlo Performance Benchmark for Detailed Power Density Calculation in a Full Size Reactor Core," Tech. rep., NEA/OECD (2011), benchmark specifications Revision 1.2, July 2011.
8. J. LEPPÄNEN, M. PUSA, T. VIITANEN, V. VALTAVIRTA, and T. KALTIAISENAHO, "The Serpent Monte Carlo code: Status, development and applications in 2013," *Annals of Nuclear Energy*, **82**, 142–150 (2015).